H), 2.28-1.28 (m, 12.5 H), 1.60, 1.52 (two s, 3 H, methyl); ^{13}C NMR ($CDCl_3$/75 MHz) δ 141.8, 141.5, 139.9, 139.7, 120.9, 120.6, 115.3, 114.6, 59.1, 38.8, 32.9, 32.6, 31.8, 31.2, 30.8, 29.9, 28.9, 28.4, 26.9, 26.8, 26.4, 23.4, 21.4, 17.1, 12.7; IR (neat/NaCl) 3002, 2931, 2854, 1682, 1456, 1447, 1380, 1234, 1209, 1173, 1136, 1092, 991 cm^{-1}; GCMS (PCI) *m/e* (rel intensity) 224 (M^+, 1), 162 (7), 161 (25), 125 (9), 121 (6), 105 (6), 93 (6), 85 (22), 81 (4), 76 (14), 75 (100), 73 (4), 59 (28); HRMS (EI) *m/e* calcd for $C_{14}H_{24}O_2$ 224.1776, found 224.1751. Anal. Calcd for $C_{14}H_{24}O_2$: C, 75.00; H, 10.78. Found: C, 75.37; H, 11.04.

1,7a-Bis(dimethoxymethyl)-1-methyloctahydro-1*H*-indene (15b). A 50-mL, three-neck, round-bottom flask equipped with a platinum gauze anode, carbon rod cathode, and a nitrogen inlet was charged with a solution of 0.198 g (0.88 mmol) of bis enol ether **14b** in 35 mL of a 2:8 mixture of methanol/dichloromethane. To this solution was added 1.862 g of lithium perchlorate and 0.316 mL (4.4 mmol) of 2,6-lutidine. The reaction was degassed by passing a stream of nitrogen through the solution and electrolyzed at a constant current of 13 mA until 175 C (2.2 faradays) of charge had been passed and only a small amount of the starting material remained by TLC. The reaction was diluted with water and ether, and the aqueous layer was extracted with ether. The combined organic layers were dried over $MgSO_4$, concentrated in vacuo, and chromatographed through 20 g of silica gel that was slurry-packed with 10% ether/pentane containing 1% triethylamine. Gradient elution from 10% ether/pentane to 40% ether/pentane afforded 0.112 g (44%) of the desired cyclized products. The desired products were contaminated with a small amount of aldehyde products arising from the hydrolysis of the acetals. Two diastereoisomers were separated. The major diastereoisomer was found to be the β isomer (cis isomer with respect to the carboxaldehyde dimethoxy acetal substituents), which gave a 3% NOE enhancement of the acetal proton on the carbon attached to C_1 when the acetal proton on the carbon attached to the bridgehead (C_{7a}) was irradiated. The other isomer did not exhibit this enhancement. The product was cis-fused across the bridgehead as suggested by the 1% enhancement on the methine proton attached to C_{3a} when the same proton (as the one above) was irradiated in both isomers. The spectral data of the mixture of diastereoisomers (cis and trans about the five-membered ring) were as follows: α isomer ^1H NMR ($CDCl_3$/300 MHz) δ 4.43 (s, 1 H, acetal proton), 4.27 (s, 1 H, acetal proton), 3.52, 3.49, 3.47, 3.46 (four s, 12 H, methoxy protons), 2.57-2.45 (m, 1 H, methine proton), 1.99-1.20 (m, 12 H), 0.96 (s, 3 H, methyl protons); ^{13}C NMR ($CDCl_3$/75 MHz) δ 112.8, 111.4, 58.7, 58.4, 57.8, 56.6, 54.6, 51.8, 35.6, 32.6, 25.9, 25.7, 24.1, 22.8, 19.6, 17.3; β isomer ^1H NMR ($CDCl_3$/300 MHz) δ 4.30 (s, 1 H, acetal proton), 4.12 (s, 1 H, acetal proton), 3.53, 3.52, 3.49, 3.44 (four s, 12 H, methoxy protons), 2.60-2.49 (m, 1 H, methine protn at C3a), 1.95-1.20 (m, 12 H), 0.93 (s, 3 H, methyl protons); ^{13}C NMR ($CDCl_3$/75 MHz) δ 113.0, 59.5, 59.4, 57.1, 56.6, 56.1, 51.2, 38.7, 31.2, 27.2, 26.6, 26.3, 23.0, 20.3, 18.6; IR (neat/NaCl) α and β isomers 2928, 2876, 1465, 1440, 1375, 1188, 1103, 1072, 969, 915 cm^{-1}; GCMS (PCI) *m/e* (rel intensity) 285 ($M^+ - 1$, 1), 253 (5), 224 (8), 223 (54), 221 (9), 191 (12), 159 (9), 149 (9), 89 (7), 76 (11), 75 ($(CH_3O)_2CH^+$, 100), 74 (10), 61 (11); HRMS (EI) *m/e* calcd for $C_{15}H_{27}O_3$ ($M^+ - OCH_3$) 255.1960, found 255.1958.

Acknowledgment. This work was supported by Washington University, the donors of the Petroleum Research Fund, administered by the American Chemical Society, the Biomedical Research Support Program, Division of Research Resources, National Institutes of Health, and the National Science Foundation (CHE-9023698). We also gratefully acknowledge the Washington University High Resolution NMR Facility, partially supported by NIH 1S10R02004, and the Washington University Mass Spectrometry Resource Center, partially supported by NIHRR00954, for their assistance.

Molecular Structure and Intramolecular Motion of (*E*)-Stilbenes in Crystals. An Interpretation of the Unusually Short Ethylene Bond

Keiichiro Ogawa,* Takashi Sano,† Shin Yoshimura, Yoshito Takeuchi, and Koshiro Toriumi‡

Contribution from the Department of Chemistry, The College of Arts and Sciences, The University of Tokyo, Komaba, Meguro-ku, Tokyo, 153 Japan, and Institute for Molecular Science, Okazaki National Research Institutes, Myodaiji, Okazaki, 444 Japan.
Received June 13, 1991. Revised Manuscript Received September 26, 1991

Abstract: Crystal structures of (*E*)-2,2′-dimethylstilbene (**2**), (*E*)-2,2′,4,4′-tetramethylstilbene (**3**), (*E*)-2,2′,5,5′-tetramethylstilbene (**4**), (*E*)-2,2′,4,4′,5,5′-hexamethylstilbene (**5**), and (*E*)-2,2′,3,3′-tetramethylstilbene (**6**) were determined at several temperatures by X-ray diffraction. Analyses of these results and also of those reported for (*E*)-stilbene (**1**) and its related compounds revealed that the X-ray structures of compounds having the (*E*)-stilbene skeleton commonly show an unusually short bond length for the ethylene bond and a strong temperature dependence for the molecular structure. No sign confirming these anomalies could be detected in solution by NMR or UV spectroscopy. It is concluded that the short ethylene bond in the X-ray structures of these compounds is an artifact caused by dynamic averaging originating from the torsional vibration of the C–Ph bonds, during which the movement of the benzene rings is restrained to be a minimum. The observed temperature dependence of the ethylene bond length and angles and of the torsion angles of the C–Ph bonds is ascribed to the slight energy difference between the conformers, which interconvert by the torsional vibration. It has also been revealed that the rotational vibration of the benzene rings around the normal axes through C1 and C1′ is a characteristic motion of (*E*)-stilbenes in the crystalline state.

Introduction

(*E*)-Stilbene (**1**) is a well-known compound which has been extensively studied for a long time in various areas of chemistry, and much effort has been devoted to understanding its ground- and excited-state properties.[1] The molecular geometry is, however, still not unambiguously established, because the ethylene bond was observed to be unusually short by X-ray diffraction.[2-6]

† On leave from Mitsubishi Oil Co., Ltd., Ohgimachi, Kawasaki-ku, Kawasaki, 210 Japan.

‡ Okazaki National Research Institutes. Present address: Department of Material Science, Faculty of Science, Himeji Institute of Technology, Harima Science Park City, Kamigori, Hyogo, 678-12 Japan.

(1) For our recent work: Ogawa, K.; Suzuki, H.; Higuchi, J.; Tajima, K.; Ishizu, K. *Bull. Chem. Soc. Jpn.* **1990**, *63*, 1816-1818. Ogawa, K.; Futakami, M.; Suzuki, H.; Kira, A. *J. Chem. Soc., Perkin Trans. 2* **1988**, 2115-2118.

(2) Robertson, J. M.; Woodward, I. *Proc. R. Soc. London, Ser. A* **1937**, *162*, 568-583.

(3) Finder, C. J.; Newton, M. G.; Allinger, N. L. *Acta Crystallogr.* **1974**, *B31*, 411-415.

0002-7863/92/1514-1041$03.00/0

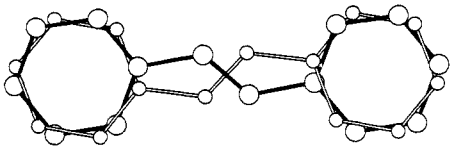

Figure 1. Orientational disorder observed for **1**.[5]

Similar phenomena were also observed in other compounds having the (*E*)-stilbene skeleton.[7-11] Considering the findings of accurate X-ray analysis that subtle differences in bond length as large as 0.02–0.03 Å can be associated with differences in stereoelectronic effects and, in some cases, with a significant change in the chemical reactivity of organic molecules,[12-14] the problem of the ethylene bond length in **1** and its related compounds is of great interest. We describe here the generality of the phenomena and their interpretation on the basis of a new model of dynamical disorder originating from the torsional vibrations of the C–Ph bonds.

The crystal structure of the parent compound **1** was first determined by Robertson and Woodward in 1937 using a photographic method.[2] The molecular structure data were frequently used for theoretical and spectroscopic investigations. To obtain more accurate geometrical data, redeterminations of the crystal structure have been repeatedly carried out.[3-6] They reveal that there are two independent molecules lying at inversion centers in the unit cell and that one of them shows an orientational disorder. The molecules at the disordered site are approximately related to one another by a 180° rotation around their longest axes, as shown in Figure 1. Due to the disorder, the ethylene bond showed an apparent shrinking as large as 0.05 Å. Similar phenomena were also found in azobenzenes and benzylideneanilines.[7]

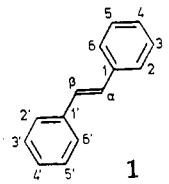

1

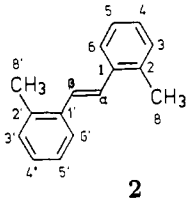

2

The ethylene bond at the nondisordered site of **1**, however, showed a length of 1.313 (4)–1.326 (2) Å at room temperature,[3-5] which is still shorter than the standard length of the ethylene bond (1.337 (6) Å),[15] but showed a nearly normal length of 1.341 (2) Å at 113 K.[6] The origin of this phenomenon has not yet been fully discussed. The shrinking of the ethylene bond without disorder was reported for many compounds having the (*E*)-stilbene skeleton.[8-10]

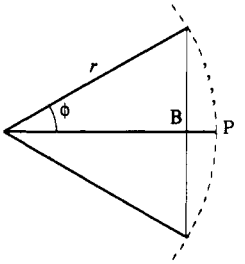

Figure 2. Displacement $\overline{PB} = r - r\cos\phi \approx r\phi^2/2$ caused by libration.[16-18]

The most remarkable example of such cases was found by Gandour and his collaborators.[10] The observed length of the ethylene bond of (*E*)-2,2′-dimethylstilbene (**2**) in the crystalline state at room temperature was 1.284 (4) Å, a value much shorter than expected for an isolated ethylene bond.

We carried out independent X-ray diffraction measurements of **2** at 296 and 118 K.[11] No disorder could be detected at either temperature from the final difference Fourier syntheses. The structure observed at 296 K was identical with the structure reported by Gandour's group. Although the structure observed at 118 K had the same crystal system as the 296 K structure, the molecular structure around the ethylene bond at 118 K was significantly different from the structure at room temperature. The length of the ethylene bond is 1.325 (2) Å at 118 K, which is ca. 0.05 Å longer than that of the 296 K structure and is still substantially shorter than the value expected for an ethylene bond conjugated with two benzene rings (1.353 Å estimated by molecular mechanics calculations).

An apparent shrink of interatomic distances that does not originate from disorder has usually been explained by libration of the molecule regarded as a rigid body around an axis through the gravity center of the molecule (the rigid-body model).[16-19] According to this model, rotational oscillations of molecules cause the apparent atomic positions to be slightly displaced from the true positions toward the rotational axes. If the root-mean-square amplitude of libration around the axis is ϕ, the radial displacement $\overline{PB}$ is given approximately by $r\phi^2/2$, where r is the distance of the atom from the axis (see Figure 2). If this model is applied to **2**, the apparent shrinking of the ethylene bond is expected to be smaller than that of the distance between C1 and C1′, because the distance of C1 (C1′) from the axis which passes the center of the ethylene bond is larger than the distance of Cα (Cβ) from the axis. The shrinking of the distance between C1 and C1′ was, however, not observed. The results for **2**, therefore, cannot be explained by the rigid-body model.

Another unusual feature of the observed molecular structure of **2** is the remarkable increase in the torsion angles of the C–Ph bonds with decreasing temperature (from 11.4° at 296 K to 18.0° at 118 K). Although the temperature dependence of torsion angles is known in other compounds,[20] its magnitude in **2** is unusually

(4) Bernstein, J. *Acta Crystallogr.* **1975**, *B31*, 1268–1271.
(5) Boustra, J. A.; Schouten, A.; Kroon, J. *Acta Crystallogr.* **1984**, *C40*, 428–431.
(6) Hoekstra, H. A.; Meertens, P.; Vos, A. *Acta Crystallogr.* **1975**, *B31*, 2813–2817.
(7) Brown, C. J. *Acta Crystallogr.* **1966**, *21*, 146–152. Brown, C. J. *Acta Crystallogr.* **1966**, *21*, 153–158. Bar, I.; Bernstein, J.; Christensen, A. *Acta Crystallogr.* **1976**, *B34*, 1609–1611. Walczak, M.; Stucky, G. *J. Am. Chem. Soc.* **1976**, *98*, 5531–5539. Bar, I.; Bernstein, J. *Acta Crystallogr.* **1978**, *B34*, 3438–3441. Valle, G.; Busetti, V.; Galiazzo, G. *Cryst. Struct. Commun.* **1981**, *10*, 867–870. Boustra, J. A.; Schouten, A.; Kroon, J. *Acta Crystallogr.* **1983**, *C39*, 1121–1123. Agostini, G.; Corvaja, C.; Giacometti, G.; Pasimeni, L.; Clemente, D. A. *J. Phys. Chem.* **1988**, *92*, 997–1003. Zobel, D.; Ruban, G. *Acta Crystallogr.* **1983**, *B39*, 638–645.
(8) Jungk, S. J.; Fronczek, F. R.; Gandour, R. D. *Acta Crystallogr.* **1984**, *C40*, 1873–1875.
(9) Tirado-Rives, J.; Oliver, M. A.; Fronczek, F. R.; Gandour, R. D. *J. Org. Chem.* **1984**, *49*, 1627–1634. Zobel, V. D.; Ruban, G. *Acta Crystallogr.* **1978**, *B34*, 1652–1657. Butters, T.; Haller-Pauls, I.; Winter, W. *Chem. Ber.* **1982**, *115*, 578–592. Arrieta, J. M.; Dominguez, E.; Lete, E.; Villa, M. J.; Gemain, G. *Acta Crystallogr.* **1984**, *C40*, 859–861. Krohn, K.; Müller, H.; Adiwidjaja, G.; Jarchow, O. H.; Schmalle, H. W.; Hausen, B. M.; Schulz, K-H. *Z. Kristallogr.* **1986**, *174*, 283–290. Bruce, M. I.; Snow, M. R.; Tiekink, R. T. *Acta Crystallogr.* **1987**, *C43*, 1640–1641. Zobel, D.; Rugan, G. *Acta Crystallogr.* **1979**, *B34*, 1652–1657.
(10) Tirado-Rives, J.; Fronczek, F. R.; Gandour, R. D. *Acta Crystallogr.* **1985**, *C41*, 1327–1329.
(11) Ogawa, K.; Suzuki, H.; Sakurai, T.; Kobayashi, K.; Kira, A.; Toriumi, K. *Acta Crystallogr.* **1988**, *C44*, 505–508.
(12) Dunitz, J. D. *Bull. Chem. Soc. Jpn.* **1988**, *61*, 1–11.
(13) Jones, P.; Kirby, A. J. *J. Am. Chem. Soc.* **1984**, *106*, 6207–6212. Edwards, M. R.; Jones, G. P.; Kirby, A. J. *J. Am. Chem. Soc.* **1986**, *108*, 7067–7073.
(14) Ōsawa, E.; Kanematsu, K. *Molecular Structure and Energetics*; Greenberg, A., Liebman, J. F., Eds.; Verlag Chemie International, Inc.: Deerfield Beach, FL, 1986; Vol. 3, Chapter 7, pp 329–369.
(15) *International Tables for X-ray Crystallography* Kynoch Press: Birmingham, 1968; Vol. III; Present distributor D. Reidel, Dordrecht, The Netherlands.
(16) Cruickshank, D. W. J. *Acta Crystallogr.* **1956**, *9*, 757–758.
(17) Dunitz, J. D. *X-ray Analysis and the Structure of Organic Molecules*; Cornell University Press: Ithaca, NY, 1979; p 244–261.
(18) Dunitz, J. D.; Maverick, E. F.; Trueblood, K. N. *Angew. Chem., Int. Ed. Engl.* **1988**, *27*, 880–895.
(19) Dunitz, J. D.; Schomaker, V.; Trueblood, K. N. *J. Phys. Chem.* **1988**, *92*, 856–867.
(20) For example, see: Yang, Qing-Chuan; Richardson, M. F.; Dunitz, J. D. *Acta Crystallogr.* **1989**, *B45*, 312–323. Brock, C. P.; Morelan, G. L. *J. Phys. Chem.* **1986**, *90*, 5631–5640. Busing, W. R. *Acta Crystallogr.* **1983**, *A39*, 340–347.

large for crystals which do not show phase transitions.

To disclose the generality and the origin of the unusual features of the molecular structures of **1** and **2**, the structures of **2** and a series of its related compounds, (*E*)-2,2′,4,4′-tetramethylstilbene (**3**), (*E*)-2,2′,5,5′-tetramethylstilbene (**4**), (*E*)-2,2′,4,4′,5,5′-hexamethylstilbene (**5**), and (*E*)-2,2′,3,3′-tetramethylstilbene (**6**), have been studied by X-ray crystallography and NMR and electronic absorption spectroscopy, and the literature data on **1** and its related compounds have been examined.

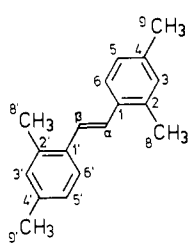

3

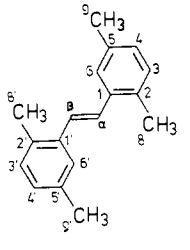

4

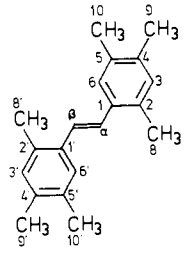

5

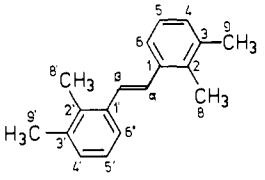

6

Experimental Section

Melting points were determined on a hot-stage apparatus and are uncorrected. NMR spectra were recorded on a Varian EM-390 or JEOL GX-270 spectrometer. UV spectra were recorded on a JASCO Ubest-50 spectrometer. For the low-temperature UV spectra, an Oxford Instruments liquid nitrogen cryostat DN1704 was used. Tetrahydrofuran (THF) was dried by distillation under argon from sodium. *N,N*-Dimethyl[*carbonyl*-^{13}C]formamide was purchased from MSD Isotopes. 2,4-Dimethylbenzaldehyde, 2,4,5-trimethylbenzaldehyde, and 2,3-dimethylbenzaldehyde were prepared according to the published procedure.[21] The syntheses of (*E*)-2,2′-dimethylstilbene (**2**) (mp 81.0–82.0 °C from hexane) and (*E*′)-2,2′,5,5′-tetramethylstilbene (**4**) (mp 161.0–162.0 °C from hexane) were previously reported.[22]

Synthesis of (*E*)-2,2′,4,4′-Tetramethylstilbene (3). Titanium tetrachloride (4.27 g, 22.5 mmol) was added to stirred THF (150 mL) in a flask on an external ice bath. To the resulting turbid yellow mixture was added powdered zinc (2.94 g, 45 mmol), portionwise with stirring. After all of the zinc had been added, the cold bath was removed. To the solution was added a solution of 2,4-dimethylbenzaldehyde (2.01 g, 15 mmol) in dry THF (10 mL). The resulting mixture was refluxed under nitrogen for 17 h. The reaction mixture was then allowed to slowly cool to room temperature. The reaction mixture was further cooled by application of an external ice bath, and the cooled solution was quenched via the gradual addition of a 10% aqueous sodium carbonate solution (100 mL, excess). The reaction mixture was extracted with diethyl ether (70 mL × 4). The combined ether layers were washed with brine (50 mL × 3). The organic layer was dried (anhydrous magnesium sulfate) and filtered, and the filtrate was concentration in vacuo. The residue (2.17 g) was recrystallized from methanol (60 mL), affording **3** (1.17 g, 66%) as colorless crystals, mp 109.0–109.5 °C (lit.[23] mp 107 °C).

The single crystals for the X-ray diffraction were obtained by the slow evaporation of the hexane solution at room temperature.

(*E*)-2,2′,4,4′,5,5′-Hexamethylstilbene (5). The procedure was the same as for the preparation of **3** except that 2,4,5-trimethylbenzaldehyde was used instead of 2,4-dimethylbenzaldehyde: colorless crystals, mp 168.5–169.5 °C. Anal. Calcd for $C_{20}H_{24}$: C, 90.85; H, 9.15. Found: C, 91.06; H, 8.91. The single crystals of **5** for the X-ray diffraction were obtained by slow evaporation of the cyclohexane solution at room temperature.

(*E*)-2,2′,3,3′-Tetramethylstilbene (6) was prepared according to the same procedure as **3** except that 2,3-dimethylbenzaldehyde was used instead of 2,4-dimethylbenzaldehyde: colorless crystals, mp 144.0–145.0 °C (lit.[24] mp 144.1–144.8 °C). The single crystals of **6** for the X-ray diffraction were obtained by slow evaporation of the hexane solution at room temperature.

(*E*)-2,2′-Dimethyl[α,β-$^{13}C_2$]stilbene (^{13}C-2). A solution of *o*-bromotoluene (1.28 g, 7.5 mmol) in THF (10 mL) was slowly added to magnesium turnings (0.27 g, 11 mmol) in THF (10 mL) under argon at 70 °C. The mixture was stirred for 0.5 h and allowed to cool to room temperature with continuous stirring. To the solution was slowly added a solution of *N,N*-dimethyl[*carbonyl*-^{13}C]formamide (0.50 g, 6.7 mmol) in THF (7 mL). The resulting mixture was stirred under argon for 16 h. To the reaction mixture was added excess saturated aqueous ammonium chloride solution (30 mL). The solution was extracted three times with diethyl ether, and the combined organic layers were washed three times with brine, dried over anhydrous magnesium sulfate, and concentrated in vacuo. The residue (0.56 g) was characterized as 2-methyl-[*carbonyl*-^{13}C]benzaldehyde from NMR and IR spectra: ^{1}H NMR (90 MHz, $CDCl_3$) δ 10.16 (d, 1 H, $^1J(^{13}C, H)$), 7.8–7.6 (m, 1 H), 7.5–6.9 (m, 3 H), 2.61 (s, 3 H); IR (neat) 1662 cm^{-1} (^{13}C=O). It was immediately used in the next reaction. By employing the same procedure that was used for the preparation of **3**, ^{13}C-**2** (112 mg) was obtained as colorless crystals.

(*E*)-2,2′,5,5′-Tetramethyl[α,β-$^{13}C_2$]stilbene (^{13}C-4) was prepared by the same procedure as ^{13}C-**2** except that 2-bromo-*p*-xylene was used instead of *o*-bromotoluene.

X-ray Crystallography. All diffraction measurements were made on a Rigaku AFC-5 diffractometer with graphite-monochromated Mo Kα radiation (λ = 0.710 73 Å). A Rigaku cooling device was used except for the measurements at room temperature. For each set of measurements, the temperature was held constant within 2 K. The integrated intensities were collected in the 2θ–ω scan mode with an ω rate of 3.0 deg min^{-1}. The intensities were corrected for Lorentz and polarization effects but not for absorption. For the determination of unit cell dimensions, 40–50 reflections in the range $20 < 2\theta < 30°$ were used. For the stucture analysis of **2**, the starting parameters from the previous report were used.[11] The other structures were solved by direct method with SHELXS-86.[25] Structures were refined by the full-matrix least-squares method using the SHELXS-76[26] or XTAL system.[27] All of the hydrogen atoms were located from difference maps. All of the carbon atoms were refined anisotropically. The function $\Sigma w(|F_o| - |F_c|)^2$ was minimized, where $w = [\sigma^2(F_o) + gF_o^2]^{-1}$. Calculations of geometrical parameters and drawings of ORTEP diagrams were performed by XTAL systems.[28] Experimental data from the X-ray crystallography are summarized in Table I, while other procedure details, including unit cell dimensions, atomic coordinates, and anisotropic displacement parameters, are given in the supplementary material.

Structure Analysis of 2 Using the Dynamical Disorder Model. The molecular structure of **2** was optimized as a free molecule by the molecular mechanics calculations using the program MMP2.[29] For this calculation, the averaged geometry observed at 298 K was used as the starting geometry. The optimized molecular structure (molecule A) was placed in the crystal at 298 K. The difference Fourier map calculated from this structure gave a skeleton of another molecule (molecule B), except for C4 and C5. The positions of C4 and C5 were determined by assuming that the benzene rings were hexagonal planar. The structures of both molecules were refined isotropically, fixing the site occupation factors at 0.60:0.40 and restraining the benzene rings to a hexagonal planar conformation. All of the hydrogen atoms were placed in geometrically idealized positions. Site occupation factors were then refined by an isotropic refinement in which the two molecules were treated as separate groups. The structure was further isotropically refined by fixing the site occupation factors for the refined values (0.44:0.56). For 129 variables, R = 0.070, R_w = 0.071, g = 0.000 03, and $(\Delta/\sigma)_{max}$ = 0.379. All of the carbon atoms were then anisotropically refined, fixing all of

(21) Dale, W. J.; Starr, L.; Strobel, C. W. *J. Org. Chem.* **1961**, *26*, 2225–2227.
(22) Kobayashi, T.; Suzuki, H.; Ogawa, K. *Bull. Chem. Soc. Jpn.* **1982**, *55*, 1734–1738.
(23) Saint-Ruf, G.; Buu-Hoi, N. P. *Bull. Soc. Chim. Fr.* **1970**, 525–527.
(24) Carruthers, W.; Stewart, H. N. M. *J. Chem. Soc., C* **1967**, 556–560.
(25) Sheldrick, G. M. *SHELXS-86*; University of Göttingen: Göttingen, Germany, 1986.
(26) Sheldrick, G. M. *SHELXS-76*; University of Cambridge: Cambridge, England, 1976.
(27) Hall, S. R.; Sterwart, J. M. *XTAL2.6*, *XTAL3.0*; Universities of Western Australia and Maryland: Nedlands, Australia, and College Park, MD, 1989, 1990.
(28) Johnson, C. K. ORTEP. Report ORNL3794; Oak Ridge National Laboratory: Oak Ridge, TN, 1965.
(29) Allinger, N. L. *MMP2* QCPE.

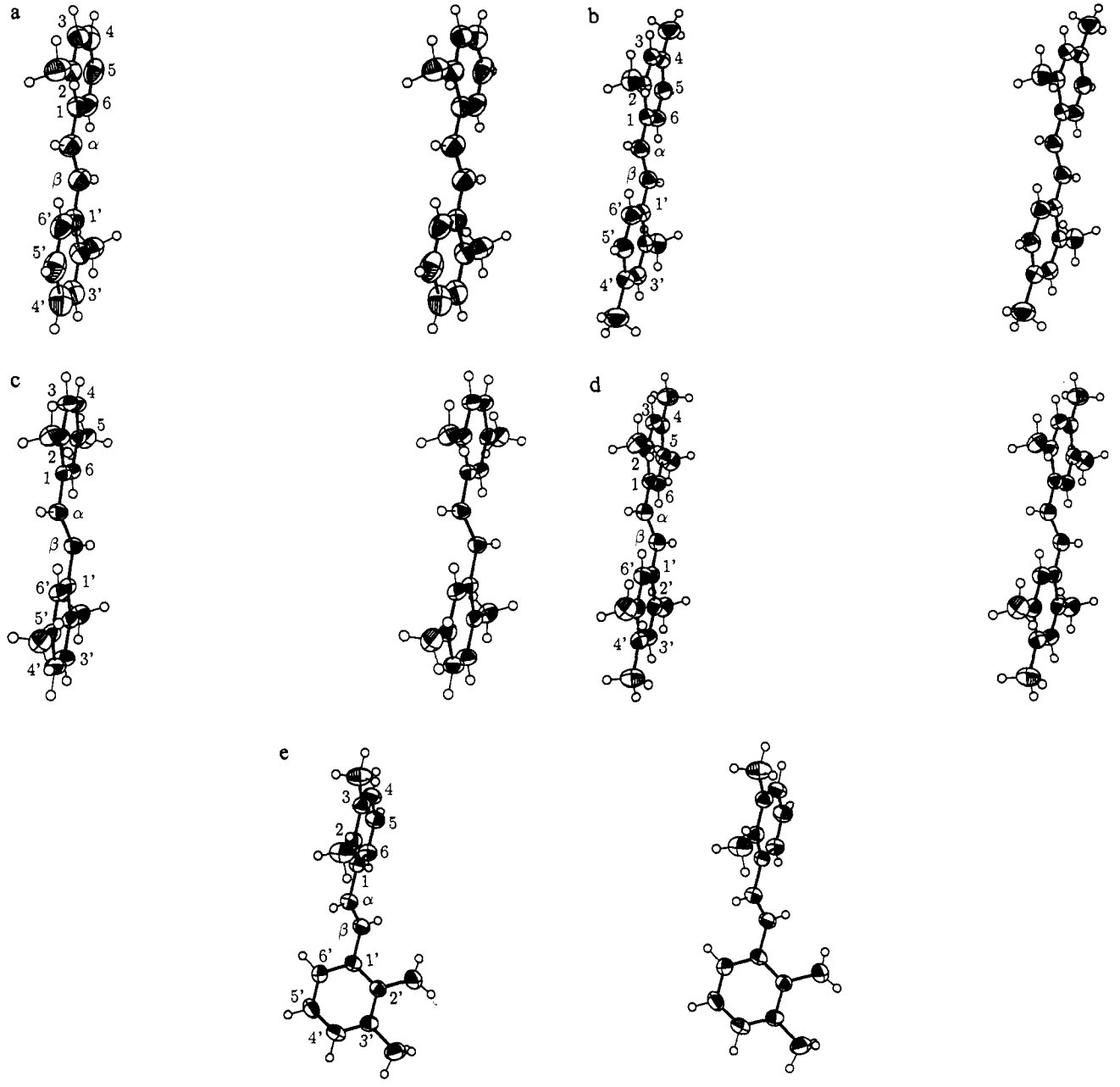

Figure 3. Stereoscopic views of the molecules of **2**–**6**: a, **2** at 298 K; b, **3** at 292 K; c, **4** at 298 K; d, **5** at 298 K; e, **6** at 298 K.

the atomic coordinates for the isotropically refined positions. For 113 variables, $R = 0.048$, $R_w = 0.044$, $g = 0.000\,05$, and $(\Delta/\sigma)_{max} = 0.228$.

For the 118 K data, difference Fourier maps calculated from the MMP2 structure could not give the second molecule. However, the refinement using the coordinates of the disordered structure at 298 K could be successfully accomplished. The refined site occupation factors were 0.70:0.30. For the final isotropic refinement with 129 variables, $R = 0.045$, $R_w = 0.054$, $g = 0.0001$, and $(\Delta/\sigma)_{max} = 0.296$. For the final anisotropic refinement with 113 variables, $R = 0.037$, $R_w = 0.044$, $g = 0.0001$, and $(\Delta/\sigma)_{max} = 0.127$.

^{13}C NMR Spectra. **2** in CD_2Cl_2: (270 MHz) δ 137.20 (C1), 135.81 (C2), 130.64 (C6), 128.35 (C5), 127.74 (C7), 125.50 (C4), 126.00 (C3), 19.84 (Me). **4** in CD_2Cl_2: (270 MHz) δ 136.83 (C1), 135.55 (C5), 132.84 (C2), 130.38 (C3), 128.33 (C4), 128.09 (C7), 126.32 (C6), 21.07 (Me), 19.47 (Me).

Digital resolution of the ^{1}H nondecoupled ^{13}C NMR spectra of ^{13}C-**2** and ^{13}C-**4** was 0.07 Hz. The spectra were analyzed by the programm DAISY.[30] The final agreement factor for the calculated and the observed spectra of ^{13}C-**2** and ^{13}C-**4** were 2.2 and 1.3%, respectively. Detailed data on the spectra are given in the supplementary material.

(30) Hägele, G.; Engelhardt, M.; Beonigk, W. *QCPE Bull.* (QCPE518) **1986**, *6*, 101.

Results and Discussion

X-ray Crystallographic Study. X-ray diffraction measurements of the crystals of **2**–**6** were carried out at several temperatures. Selected geometrical parameters are listed in Table II. Stereoscopic views of the molecules are shown in Figure 3.

All of the crystals belong to centrosymmetric space groups. The three structural isomers **3**, **4**, and **6** have nearly the same cell volume, as shown in Table I. Cell volume per molecule (V/Z) increases as the number of the methyl groups is increased. The cell volume increment per methyl group is about 20 Å^3.

The unit cell volumes for all of the crystals decreased monotonically as the temperature was lowered. All of the cell lengths decreased nearly isotropically except for **6**, in which a increased as the temperature was lowered. All of the molecules are centrosymmetric except for the molecule of **6**, which is asymmetric. In all cases, the structures were unambiguously determined and smoothly converged. The probability density function (pdf) ellipsoids of any carbon atoms show no marked anomaly, and the final difference Fourier syntheses gave no residual atom.

Features of the Observed Molecular Structures. The observed length of the ethylene bond Cα–Cβ (d) of **2**–**6** depends on the

Table I. Crystallographic Data for **2**–**6**

compd	**2**			**3**			**4**		**5**	**6**	
formula	$C_{16}H_{16}$			$C_{18}H_{20}$			$C_{18}H_{20}$		$C_{20}H_{24}$	$C_{18}H_{20}$	
space group	$P2_1/n$			$P2_1/n$			$P2_1/n$		$P\bar{1}$	$P\bar{1}$	
Z	2			2			2		1	2	
temp (K)	118[a]	175	298	123	207	292	123	298	298	121	298
V (Å^3)	606.0 (2)	611.4 (2)	618.1 (2)	679.2 (2)	691.3 (2)	704.7 (3)	662.6 (2)	687.1 (2)	396.14 (7)	680.5 (3)	701.7 (1)
max 2θ (deg)	80	75	70	65	65	65	65	65	60	70	60
no. unique refl.	1929	1692	1545	1436	1066	838	1965	1471	1581	4273	2594
no. variables	105	145	145	122	122	122	122	122	139	243	243
R	0.044	0.050	0.054	0.049	0.047	0.050	0.042	0.055	0.062	0.045	0.048
R_w	0.051	0.058	0.061	0.054	0.053	0.052	0.057	0.061	0.071	0.057	0.064
resid dens (e Å^{-3})	0.43	0.34	0.23	0.33	0.21	0.16	0.15	0.37	0.24	0.48	0.25
g[b]	−0.23	−0.27	−0.25	−0.33	−0.18	−0.16	−0.16	−0.22	−0.26	−0.23	−0.23
	0.000 111	0.000 421	0.000 431	0.000 010	0.000 237	0.000 248	0.000 250	0.000 400	0.0002	0.0001	0.000 287	0.000 200

[a] Diffraction data from ref 11. [b] Weighting scheme.

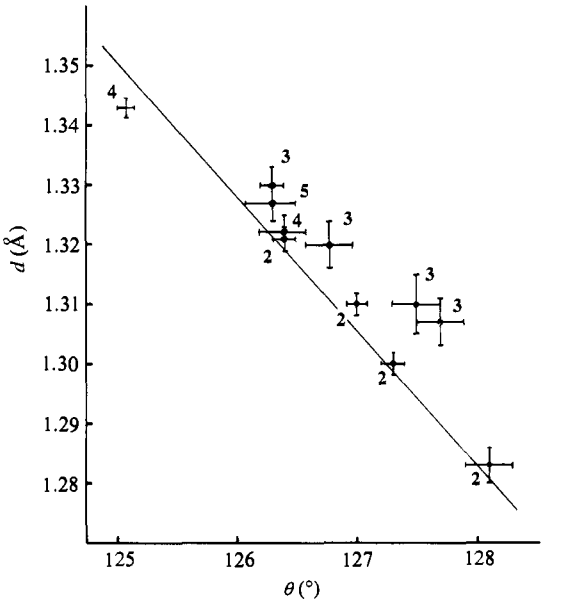

Figure 4. Plot of d vs θ. The line represents the correlation between d and θ calculated from the dynamical disorder model.

compounds and on the temperature, varying from 1.283 (3) to 1.343 (2) Å. At room temperature, the d value of **2** is the shortest (1.283 (3) Å) and the d's of **5** and **6** are the longest (1.327 (2–3) Å). The d value for any of the compounds is always shorter than the standard length of an isolated C=C bond (1.337 (6) Å) at room temperature, and it significantly increases as the temperature is lowered. At low temperature, the d value of **2** (1.321 (2) Å) is the shortest, and d for **4** is the longest (1.343 (2) Å). It is to be noted that even at ca. 120 K, the d values are still shorter than those predicted by the molecular mechanics calculations using the program MMP2, which gave nearly identical values (1.353–4 Å) for the ethylene bonds of compounds **2**–**6**.

The length of the C–Ph bonds (average 1.473 Å) and the distance between C1 and C1′ (average 3.878 Å) are nearly the same for all of the compounds at all temperatures. The lengths of the other bonds are increased to a smaller extent than that of the ethylene bond upon lowering the temperature. Each of the C–C bond lengths observed at low temperature except the ethylene bond agrees with the corresponding values predicted by MMP2 calculations within ±0.011 Å.

All of the observed C–C–C bond angles, except Cβ–Cα–C1 and Cα–Cβ–C1′, are normal and show marginal temperature dependence: The values observed at low temperature agree with the corresponding values predicted by the MMP2 calculations within ±1.1°. The magnitudes of angles Cβ–Cα–C1 and Cα–Cβ–C1′ (θ), in contrast, substantially deviate from the values predicted by the MMP2 calculations and show significant temperature dependence in all cases. They decrease as the temperature is lowered. The correlations between d and θ are approximately linear for all of the compounds except **6** in the observed temperature range, as shown in Figure 4: the smaller d is, the larger θ is.

The magnitudes of the observed torsion angles of Cβ–Cα–C1–C6 and Cα–Cβ–C1′–C6′ (ω's) strongly depend on the compounds and the temperature, varying from 11.7 (3)° to 40.2 (2)° in absolute values. Two compounds, **4** and **5**, give nearly identical $|\omega|$'s of ca. 25°, which is nearly equal to the value obtained from the MMP2 calculations. Two other compounds, **2** and **3**, show $|\omega|$'s much smaller than those of **4** and **5**. For **2**–**5**, the $|\omega|$ values increase as the temperature is lowered. The largest and the smallest increase in $|\omega|$ are for **2** (6.3° from 298 to 118 K) and for **4** (1.3° from 298 to 123 K), respectively.

The molecular structure of **6** is asymmetric and has two $|\omega|$'s of ca. 25° and ca. 40°. Since the two $|\omega|$ values have the same sign, the molecular structure of **6** has a pseudo C_2 symmetry with a C_2 axis perpendicular to the ethylene plane. The larger of the

Table II. Selected Geometrical Parameters for **1–6**

compd	origin	T (K)	distance (Å) Cα–Cβ	distance (Å) C1–Cα C1′–Cβ	bond angle (deg) C1–Cα–Cβ C1′–Cβ–Cα	torsion angle (deg) C6–C1–Cα–Cβ C6′–C1′–Cβ–Cα	distance (Å) C1···C1′	distance (Å) Hβ···H6 Hα···H6′	distance (Å) Hα···H(8) Hβ···H(8′)
2	X-ray	298	1.283 (3)	1.473 (2)	128.3 (1)	±11.7 (3)	3.876 (3)	2.20 (3)	2.33 (3)
		234	1.300 (2)	1.474 (2)	127.3 (1)	±13.6 (2)	3.876 (2)	2.17 (2)	2.33 (2)
		175	1.310 (2)	1.472 (2)	127.0 (1)	±15.4 (2)	3.877 (2)	2.18 (2)	2.33 (2)
		118[a]	1.321 (2)	1.474 (1)	126.4 (1)	±18.0 (2)	3.880 (2)	2.20 (2)	2.29 (2)
	MMP2		1.353	1.478	124.9	±25.6	3.890	2.18	2.43
3	X-ray	321	1.307 (4)	1.470 (3)	127.7 (2)	±13.6 (4)	3.880 (4)	2.16 (3)	2.36 (4)
		292	1.314 (5)	1.469 (3)	127.5 (2)	±13.5 (4)	3.881 (5)	2.19 (3)	2.36 (4)
		207	1.320 (4)	1.471 (3)	126.8 (2)	±15.1 (3)	3.880 (4)	2.17 (3)	2.38 (3)
		123	1.330 (3)	1.469 (2)	126.3 (1)	±15.7 (2)	3.877 (3)	2.20 (3)	2.38 (3)
	MMP2		1.354	1.476	124.9	±25.8	3.888	2.19	2.43
4	X-ray	298	1.322 (3)	1.475 (2)	126.3 (2)	±25.9 (2)	3.883 (3)	2.32 (3)	2.48 (3)
		123	1.343 (2)	1.472 (1)	125.1 (1)	±27.6 (1)	3.876 (2)	2.27 (2)	2.41 (2)
	MMP2		1.354	1.477	124.8	±26.0	3.889	2.18	2.43
5	X-ray	298	1.327 (3)	1.470 (2)	126.3 (2)	±25.0 (3)	3.876 (2)	2.28 (2)	2.49 (3)
	MMP2		1.354	1.477	125.1	±25.6	3.892	2.28	2.49
6	X-ray	298	1.326 (2)	1.477 (2)	126.3 (1)	25.3 (2)	3.876 (2)	2.25 (2)	2.16 (3)
				1.476 (2)	124.8 (1)	40.2 (2)		2.42 (3)	2.31 (3)
		121	1.342 (1)	1.479 (1)	125.40 (9)	28.4 (1)	3.881 (2)	2.13 (2)	2.16 (2)
				1.479 (1)	123.88 (9)	40.0 (1)		2.44 (2)	2.23 (2)
	MMP2[b]		1.353	1.478	124.5	30.8	3.886	2.23	2.35
1	X-ray	rt[c]	1.318 (5)	1.469 (4)	126.7 (3)	±5.0 (3)	3.872 (5)		
		295[d]	1.326 (3)	1.471 (2)	126.7 (2)	±5.3 (2)	3.878 (3)		
		113[e]	1.341 (2)	1.471 (2)	126.0 (1)	±6.6 (1)	3.884 (2)		
	MMP2		1.356	1.474	126.1	±0.3	3.905	2.12	

[a] Refined using the diffraction data of ref 11. [b] C_2 symmetry was assumed. [c] Room temperature; ref 3. [d] Reference 5. [e] Reference 6.

Table III. Selected Geometrical Parameters for **2** Calculated from the Disorder Model

population[a] (%)	distance (Å) Cα–Cβ	distance (Å) C1–Cα	bond angle (deg) C1–Cα–Cβ	torsion angle (deg) C6–C1–Cα–Cβ	distance (Å) C1···C1′
65	1.281	1.476	128.1	8.9	3.877
70	1.287	1.477	127.8	11.8	3.878
75	1.294	1.477	127.5	14.7	3.879
80	1.303	1.477	127.1	17.5	3.881
85	1.313	1.477	126.6	20.3	3.883
90	1.325	1.477	126.1	22.9	3.885
95	1.338	1.477	125.5	25.5	3.887
100	1.353	1.478	124.9	28.0	3.890

[a] Population of **2+**. The sum of the populations of **2+** and **2–** amounts to 100%.

$|\omega|$ values of **6**, 40°, is remarkably larger than those of the other compounds, suggesting a buttressing effect[31] caused by the methyl groups on the meta carbons. This tendency was reproduced by the MMP2 calculations (30.8°). The temperature dependence of the $|\omega|$'s of **6** is different from that of the others. While one of the $|\omega|$'s increases from 25.3 to 28.4°, the other remains almost constant with a temperature decrease from 298 to 121 K.

The nonbonding distance between the hydrogen atom on Cβ (denoted as Hβ) and the hydrogen atom on C6 (denoted as H6) is shorter than or approximately equal to the sum of the van der Waals radii.[32] The distance between Hα and a hydrogen atom of the methyl group on C2 is also shorter than or approximately equal to the sum of the van der Waals radii and is always longer than the distance between Hβ and H6, except for **6**.

Dynamical Disorder Model. The features of the observed molecular geometry (the shortening of the ethylene bond, the enlarging of the ethylene bond angle, and the flattering of the molecule) could not be explained in a chemically and physically reasonable way if it were regarded as the "true" molecular geometry.

A careful inspection of the orientation of the pdf ellipsoids of the ethylene carbons of **2** reveals that their longest axes are nearly perpendicular to the molecular plane (see Figure 3). This observation suggests that there would be an unresolved disorder which does not show strong residual peaks in the difference density maps and/or vibrations in the direction nearly perpendicular to the molecular plane. Such a disorder and/or vibrations can be most readily caused by the torsional vibration of the C–Ph bonds, during which the orientations of the benzene rings to the crystal lattice do not change but those of the ethylene unit do. In other words, the movement of the benzene rings is restrained to be as small as possible in the torsional vibration. Such a torsion motion causes an interconversion between enantiomeric conformers for the centrosymmetric molecules, **2–5**. The enantiomeric conformers must have the same energy as free molecules, but this is not necessary in the crystalline state. The observed crystal structure would be an average of both conformers with temperature-de-

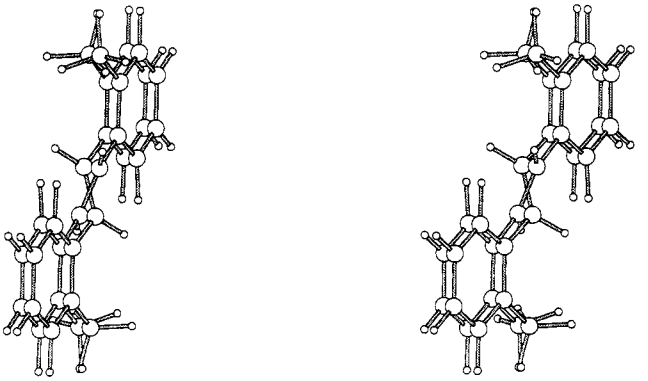

Figure 5. Stereo picture of the disorder model for **2**, drawn by the program MindTool.[33]

(31) Eliel, E. R. *Stereochemistry of Carbon Compounds*; McGraw-Hill, Inc.: New York, 1962; Chapter 6. Theilacker, W.; Böhm, H. *Angew. Chem., Int. Ed. Engl.* **1967**, *6*, 251.
(32) C. 1.70; H, 1.20 Å: Bondi, A. *J. Phys. Chem.* **1954**, *68*, 441–451.
(33) Tirado-Rives, J.; Blake, J. *MindTool*; Yale University: New Haven, CT, 1990.

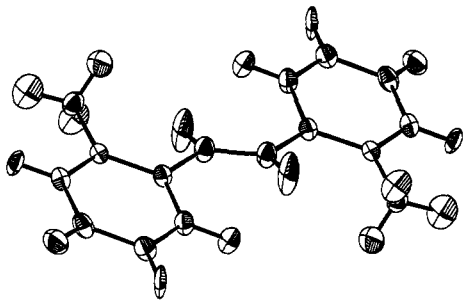

Figure 6. ORTEP drawing of the averaged structure of **2** at 118 K.

pendent, unequal site occupation factors.

Figure 5 shows a stereo picture of a superposition of enantiomeric conformers of **2** designated as **2+** and **2−**, whose structures are assumed to be "true". The torsion angles of Cβ–Cα–C1–C6 and Cα–Cβ–C1′–C6′ in **2+**, of which the geometry was optimized by the MMP2 calculations, were set at +28° and −28°, respectively. The corresponding torsion angles of **2−** are −28° and +28°, respectively. The two conformers are interrelated by reflection with the plane which is parallel with the benzene rings and passes the center of the ethylene bond.[34] Table III shows the averaged geometry of these conformers with various site occupation factors.

Figure 5 and Table III reproduce well the features of the observed molecular geometry and of the orientation of pdf ellipsoids. All of the corresponding C–C bonds parallel or nearly parallel each other, except the ethylene bonds which cross each other at the center of the bond. All of the C–C bond lengths and C–C–C bond angles of the averaged structure are, therefore, equal or nearly equal to the corresponding ones of the true structure, except the bond length of Cα–Cβ and bond angles of Cβ–Cα–C1 and Cα–Cβ–C1′. The bond length Cα–Cβ and angles Cβ–Cα–C1 and Cα–Cβ–C1′ of the averaged stucture are substantially shorter and larger than the corresponding ones of the true structure, respectively. The distance between C1 and C1′ of the averaged structure is slightly shorter than that of the true structure. The torsion angles Cβ–Cα–C1–C6 and Cα–Cβ–C1′–C6′ of the averaged structure are 0° if the two true structures have equal site occupation factors but deviate from 0° for unequal site occupation factors.

According to this model, the pdf ellipsoids of all of the carbon atoms would have orientations in which the longest axes are nearly perpendicular to the molecular plane. Since the separation between the corresponding ethylene carbons (ca. 0.45 Å) is slightly larger than that of the other carbon atoms (ca. 0.33 Å), the mean-square displacement amplitude (MSDA) of Cα in this direction would be accordingly larger than that of other carbon atoms and that of the hydrogen atom on Cα would be still larger. These features are in fair agreement with the observed ones (see Figures 3a and 6).

The above discussions were confirmed by the successful refinement of the crystallographic data of **2** using the disorder model. Thus, the difference Fourier maps obtained after locating the MMP2 structure (molecule A) in the crystal gave the second molecule (molecule B) for 298 K data. The crystal structure at 118 K could also be refined using the disordered structure at 298 K, although the second molecule could not be located by difference Fourier syntheses. The site occupation factors changed by ca. 26% with the temperature decrease from 298 to 118 K. Figure 7 clearly shows that the results are in essential agreement with the results obtained from the calculated disorder model.

The temperature dependence of the site occupation factors was roughly estimated by the comparison of the averaged observed geometries at different temperatures (Table II) with the geometries obtained from the calculated disorder model (Table III). Thus, the ratio **2+**:**2−** is approximately equal to 0.65:0.35 at 298 K, 0.80:0.20 at 234 K, 0.85:0.15 at 175 K, and 0.90:0.10 at 118 K.

(34) The geometry of the averaged structure is very sensitive to the values of torsion angles Cβ–Cα–C1–C6 and Cα–Cβ–C1′–C6′. The use of values ±28° best reproduced the observed geometry.

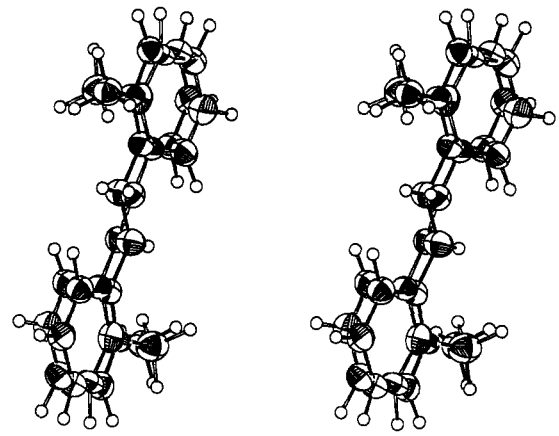

Figure 7. Composite view of the disordered molecules of **2** at 298 K.

Table IV. U_{eq} Values of the Carbon Atoms of the (*E*)-Stilbene Skeleton

$$U_{eq} = \tfrac{1}{3}\sum_i\sum_j U_{ij}a^*_i a^*_j \mathbf{a}_i\mathbf{a}_j$$

		U_{eq}						
compd	*T* (K)	C1 C1′	C2 C2′	C3 C3′	C4 C4′	C5 C5′	C6 C6′	Cα Cβ
2	118	0.0193	0.0181	0.0209	0.0243	0.0245	0.0230	0.0254
	298	0.0519	0.0509	0.0610	0.0718	0.0732	0.0644	0.0638
3	123	0.0175	0.0167	0.0192	0.0199	0.0201	0.0198	0.0197
	321	0.050	0.050	0.058	0.058	0.063	0.059	0.059
4	123	0.0117	0.0123	0.0151	0.0152	0.0129	0.0131	0.0131
	298	0.0317	0.0337	0.0426	0.0429	0.0359	0.0353	0.0361
5	298	0.0399	0.0420	0.0468	0.0462	0.0435	0.0441	0.0438
6	121	0.0141	0.0148	0.0153	0.0167	0.0181	0.0166	0.0158
		0.0148	0.0147	0.0152	0.0176	0.0192	0.0178	0.0167
	298	0.0396	0.0413	0.0449	0.0496	0.0519	0.0472	0.0434
		0.0406	0.0412	0.0440	0.0498	0.0545	0.0494	0.0456

From these data, the enthalpy difference between the enantiomers is estimated to be ca. 0.6 kcal mol^{-1} in the crystals. A variation in the observed geometry with a change of temperature, i.e., that of the site occupation factor, was completely reversible. The energy barrier for the interconversion between the enantiomers would not be much higher than the barrier for the free molecule, which was estimated as ca. 0.7 kcal mol^{-1} by the MMP2 calculations. In addition, all of the pdf ellipsoids become distinctly smaller with decreasing temperature, as clearly seen from Figures 3a and 6 and Table IV. It is therefore concluded that the disorder mainly originates from the torsional vibration of the C–Ph bonds.

The calculated disorder model approximately reproduces the observed averaged geometries not only of **2** but also of **3**–**5** at various temperatures (see Tables II and III and Figure 4). Therefore, the true geometry around the ethylene unit of **2**–**5** could be inferred to be nearly equal to the MMP2 geometry, which is nearly the same for these compounds. Thus, in the true geometry of **2**–**5**, the bond length of Cα–Cβ would be ca. 1.35 Å, bond angles Cβ–Cα–C1 and Cα–Cβ–C1′ would be 125°, and torsion angles Cβ–Cα–C1–C6 and Cα–Cβ–C1′–C6′ would be ca. 28° and −28°, respectively.

The disorder model does not hold for **6** because its observed structure has a pseudo-C_2 symmetry. The results for **6** can be explained by the following model. If the true torsion angles Cβ–Cα–C1–C6 and Cα–Cβ–C1′–C6′ of **6** are tentatively assumed to be 20° and 45°, respectively, then a conformer with 45° and 20° must have the same energy as a free molecule, but this is not necessary for the crystal. The observed crystal structure would be an average of both conformers with temperature-dependent, unequal site occupation factors. Figure 8 shows a stereo picture of a superposition of both conformers. According to this model, the averaged structure has a shortened Cα–Cβ bond and widened Cβ–Cα–C1 and Cα–Cβ–C1′ angles, and the resulting pdf ellipsoids of the carbon atoms have orientations similar to the observed ones. One of the torsion angles in the averaged structure increases and the other decreases with variation of the site occupation

Table V. Matrix of Δ Values (pm^2) for **2** at 118 K[a]

atom	C8′	Cβ	C6′	C5′	C4′	C3′	C2′	C1′	C8	Cα	C6	C5	C4	C3	C2
C1	47	15	43	44	−1	7	13	0	−5	6	3	−6	−8	6	3
C2	35	6	28	51	−4	−7	0	−13	−2	2	−3	−14	−9	4	
C3	45	9	32	50	−3	0	7	−7	−14	3	−4	−3	−1		
C4	29	8	54	56	0	3	4	1	−2	14	2	6			
C5	−23	−35	16	0	−56	−50	−51	−44	11	−11	−4				
C6	25	−35	0	−16	−54	−32	−28	−43	−2	−29					
Cα	15	0	35	35	−8	−9	−6	−15	9						
C8	0	−15	−25	23	−29	−45	−35	−47							

[a] Each Δ value is the MSDA for the atom at the head of column minus the MSDA for the atom at the left end of the row, each MSDA being measured along the vector between the atoms (see eq 1). For triangles A (right) and B (left), see the text.

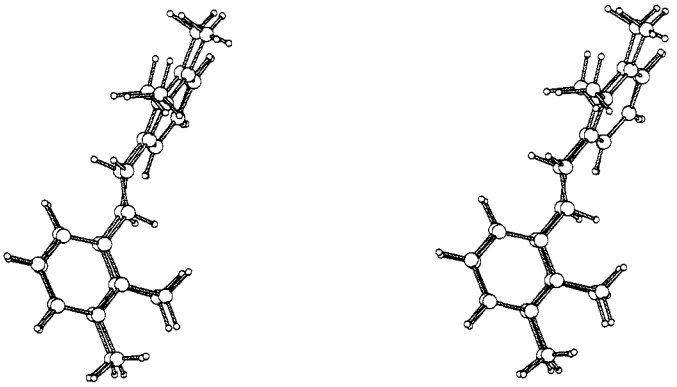

Figure 8. Stereo picture of the disorder model for **6**.

factors. Thus, the disorder model qualitatively reproduces the observed results.

This disorder must also originate from the torsional vibration of the C–Ph bonds, during which the movement of the benzene rings is restrained to a minimum. The planar conformation is not passed through in the torsional vibration of **6**, in sharp contrast with that of **2–5**.

ADP Analyses. Evidence for a large amplitude relative motion of the two benzene rings in a molecule is also given by the ADP analyses using the program THMA11.[35] When $z^2_{A,B}$ is the MSDA of atom A in the direction of atom B and $z^2_{B,A}$ is the MSDA of atom B in the direction of atom A, the difference between the two quantities as expressed in eq 1 serves as a good criterion for the rigidity of subgroups in a molecule.[12,19] For atoms in a

$$\Delta = z^2_{A,B} - z^2_{B,A} \quad (1)$$

perfectly rigid grouping, Δ must be zero. The relative motion of the subgroups is suggested by the large deviations from zero of some of the intergroup Δ values.

Table V shows Δ values calculated for **2** at 118 K. The triangle labeled A contains Δ values corresponding to the interaction of the atoms within a benzene ring. The triangle labeled B contains Δ values corresponding to the interaction of the atoms of different rings. The root-mean-square of the Δ values for triangle A is 6.0 pm^2, which is much smaller than 33.9 pm^2 for triangle B, where 1 pm = 0.01 Å. According to Hirshfeld, in pairs of bonded atoms the Δ's should be smaller than 10 pm^2 for C–C bonds in organic molecules.[36] The benzene rings are, therefore, essentially rigid, and there is significant motion between different rings in a molecule. Essentially the same results were obtained for all of the other crystals, as shown in Table VI.

It is to be noted that some benzene ring carbon atoms show the typical pattern of the ellipsoid orientations, which indicates

Table VI. Root-Mean-Square Δ Values for the Benzene Rings (Column A) and for the Interaction of Different Rings in the Molecule (Column B)

compd	T (K)	rms of Δ (pm^2) A	B
2	118	6.0	33.9
3	123	8.1	17.4
4	123	4.5	14.0
5	298	8.1	37.2
6	121	4.3	21.7
		3.6	13.7

Table VII. Results of ADP Analyses for the Rotational Vibration of the Benzene Rings around Their Axes through C1 and C1′

compd	T (K)	R[a]	$\langle\phi^2\rangle$ (deg^2)	$\bar{\nu}$ (cm^{-1})
2	118	0.123	5.4 (2.8)	73 (15)
	175	0.124	7.1 (4.0)	76 (16)
	234	0.116	9.0 (5.2)	68 (14)
	298	0.099	12.3 (6.6)	76 (15)
3	123	0.118	5.5 (2.3)	56 (9)
	207	0.118	9.2 (4.0)	56 (9)
	292	0.103	14.8 (5.3)	52 (7)
	321	0.098	16.7 (5.7)	51 (7)
4	118	0.076	2.8 (0.7)	82 (9)
	298	0.085	8.1 (2.2)	47 (5)
5	298	0.094	12.1 (4.0)	51 (28)
6	123	0.068	3.9 (0.6)	69 (5)
			4.2 (0.6)	67 (5)
	298	0.076	9.6 (1.9)	69 (6)
			12.2 (1.9)	61 (4)

[a] $R = [\sum(\Delta U_{ij})^2/\sum(U_{ij})^2]^{1/2}$.

Table VIII. Ethylene Bond Lengths and Isotropic Displacement Parameters

compd	distance (Å) Cα–Cβ	isotropic displacement parameters ($Å^2$) quantity	C1	Cα	Cβ	C1′	ref
1	1.341 (2)	$^1/_3\sum_{i=1}^3 U_{ii}$	0.0139	0.0160			6
7	1.320 (4)	B_{eq}	3.54	3.86	4.05	3.47	8
8	1.313 (9)	B_{eq}	2.96	3.28	3.36	3.43	37
9	1.325 (8)	U_{eq}	0.0422	0.0472	0.0491	0.0457	38
10	1.315 (3)	B_{eq}	3.26	4.09	4.18	4.03	39

the additional motion in the tangential directions of the benzene rings. It also deserves attention that the U_{eq} value of C1 and C1′ is nearly the smallest of all of the carbon atoms (Table IV). U_{eq} of Cα, the carbon atom closest to the center of the molecule, is larger than that of C1 and C1′. In view of these facts, rotational vibrations of the benzene rings around their normal axes through C1 and C1′ are assumed. The THMA11 calculations using this model in which the benzene rings are treated at "attached rigid groups" best reproduced the observed ADP's for all of the cases, as shown in Table VII. The mean-square librational amplitudes $\langle\phi^2\rangle$ are essentially the same for all of the molecules at a given temperature and increase with raising the temperature. The estimated vibration frequencies are in the range 42 (5)–82 (9) cm^{-1}, which is at least of the correct order of magnitude, because this vibration involves only the bending of bond angles Cα–C1–C6(C2) and Cβ–C1′–C6′(C2′). This vibration model qualitatively reproduces the slight increase in the benzene ring bond lengths

(35) Trueblood, K. N. *Acta Crystallogr.* **1978**, *A34*, 950–954. *THMA11* K. N. Trueblood, University of California, Los Angeles, 1988.
(36) Hirshfeld, F. A. *Acta Crystallogr.* **1976**, *A32*, 239–244.
(37) Arrieta, J. M.; Lete, E.; Dominguez, E.; Germain, G.; Declerq, J. P.; Amigó, J. M. *Acta Crystallogr.* **1982**, *B38*, 3155–3157.
(38) Durant, F.; Lefèvre, F.; Bufkens, F.; Norberg, B.; Evrard, G. *Cryst. Struct. Commun.* **1982**, *11*, 1925–1932.
(39) Verbruggen, M.; Zhou, Y.; Lenstra, A. T. H.; Giese, H. J. *Acta Crystallogr.* **1988**, *C44*, 2120–2123.

and the little change in the C–Ph bond lengths of the observed averaged geometry with decreasing temperature for all of the compounds.

Discussions on 1 and Other Compounds. As shown in Table II, the observed molecular structure of **1** at the "nondisordered" site has geometrical features similar to **2–5**: a short ethylene bond and large Cβ–Cα–C1 and Cα–Cβ–C1′ bond angles. The ethylene bond length increases, the bond angles Cβ–Cα–C1 and Cα–Cβ–C1′ decrease, and the torsion angles Cβ–Cα–C1–C6 and Cα–Cβ–C1′–C6′ increase with decreasing temperature. The length of the C–Ph bonds and the distance between C1 and C1′ atoms are almost unchanged as the temperature is lowered. The longest axes of the pdf ellipsoid of all of the carbon atoms are nearly perpendicular to the molecular plane.[5] The isotropic displacement parameter of C1(C1′) is the smallest in the molecule (Table VIII). It is therefore concluded that a dynamical disorder similar to that in **2–5** is hidden at the "nondisordered site" of **1** and that a rotational vibration of the benzene rings around their normal axes through C1 and C1′ also takes place. Thus, in the true geometry of **1** in the crystalline state, the ethylene bond length would be ca. 1.35 Å, and the absolute magnitude of torsion angles Cβ–Cα–C1–C6 and Cα–Cβ–C1′–C6′ would certainly be larger than 6.6°.

A similar trend in the ethylene bond length and the isotropic displacement parameters as observed for **1–6** is also seen in other compounds having the (*E*)-stilbene skeleton such as **7–10**, for which such an orientational disorder as observed for **1** is not reported (see Table VIII). Therefore, the shortened ethylene bond

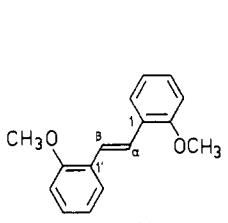

7

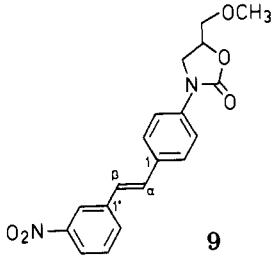

9

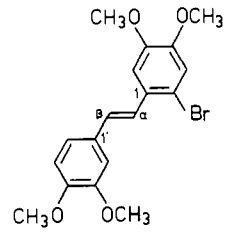

8

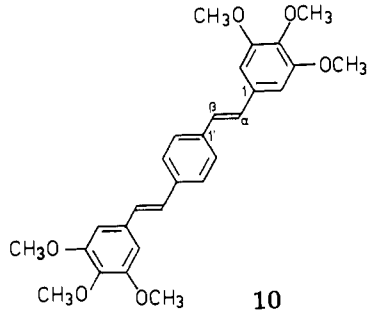

10

in these compounds may be an artifact caused by the dynamic averaging due to the torsional vibration of the C–Ph bonds, and the rotational vibration of the benzene rings around their normal axes through C1 and C1′ must take place in all of the cases.

Our conclusion seems to be consistent with the results of the spectroscopic studies of **1**. It was reported that the vibrational frequency of the ethylene bond stretching, which is closely correlated with the π bond order, was 1641 cm^{-1} and independent of the temperature in the crystalline state.[40] It hardly depends on phase (mixed crystal,[41,42] single crystal,[40] powder,[43] melt,[40] solution,[40] and gas[44-46]). Thus, the equilibrium length of the ethylene bond of **1** does not depend on temperature and phase. It was also pointed out by Edelson and Bree that the torsional mode of the C–Ph bonds is anharmonic due to intermolecular interactions.[40] Ito and his collaborators revealed that the potential of the out-of-phase torsion of the two C–Ph bonds is very anharmonic and has a flat bottom.[45] The amplitude of the torsional mode was estimated to be as large as 20° even in the zero-point level. Vibrational analyses of **2–6** must await further investigations.

Table IX. Values of s Character and ^1J of the Ethylene Carbon in **2** and **4** Calculated from the X-ray Geometries

	2 (298 K)	**4** (298 K)
s character of ψ_1[a]	0.4034	0.4089
s character of ψ_2[b]	0.3623	0.3363
s character of ψ_3[c]	0.2324	0.2548
^1J(Cα,Cβ) (Hz)	79.74	73.23
^1J(Cα,Hα) (Hz)	114.07	126.84

[a] Orbital ψ_1 is the carbon hybrid orbital which is involved in the formation of the Cα–Cβ bond. [b] Orbital ψ_2 is the carbon hybrid orbital which is involved in the formation of the Cα–C1 bond. [c] Orbital ψ_3 is the carbon hybrid orbital which is involved in the formation of the Cα–Hα bond.

Table X. Coupling Constants[a] of the Ethylene Carbons in ^{13}C-**2**, ^{13}C-**4**, and ^{13}C-**1**

	^{13}C-**2**[b]	^{13}C-**4**[b]	^{13}C-**1**
^1J(Cα,Cβ)	72.9	72.6	72.9[c]
^1J(Cα,Hα)	152.2	151.9	151.8[d]
^2J(Cα,Hβ)	(±)2.1	(±)2.0	
^3J(Cα,H6)	(±)3.4	(±)3.5	

[a] In hertz. [b] Uncertainty is 0.2 Hz. [c] Reference 56. [d] Reference 57.

NMR Study. It was confirmed by NMR and UV spectroscopy that there is no sign that indicates the unusually short length of the ethylene bond and the temperature dependence of the molecular geometry of **2–6** in solution as well as of **1**.

The carbon–carbon bond coupling constant ^1J(C, C) in the hydrocarbons strongly depends on the hybridization of the atomic orbitals of each of the two carbon atoms involved[47-51] and is roughly linear in relation to the interatomic distance.[50] It increases as the s character of the hybrid orbitals that form the C–C bond increases or the interatomic distance decreases. For example, the following empirical equation was reported:[52]

$$^1J(C_AC_B)/Hz = -167r_{AB}/Å + 294 \quad (2)$$

where r_{AB} is the distance between the two carbon atoms C_A and C_B.

Similarly, the carbon–hydrogen bond coupling constant ^1J(C, H) is sensitive to the hybridization of the atomic orbitals of the carbon atoms involved. It increases as the s character of the relevant hybrid orbital of the carbon atom increases. For example, the following empirical equation was reported:[53]

$$^1J(C, H)/Hz = 570s - 18.4 \quad (3)$$

where s is the s character of the relevant carbon hydrid orbital.

If d and θ of **2–5** in solution depend on the temperature and the compound as observed for crystals, the values of ^1J(Cα,Cβ) and ^1J(Cα,Hα) would reflect the corresponding geometry around Cα in the crystalline state. There would be a significant difference in ^1J(Cα,Cβ) and ^1J(Cα,Hα) between **2** and **4**, since there are substantial differences in d and θ between **2** and **4**. For the

(40) Edelson, M.; Bree, A. *Chem. Phys. Lett.* **1976**, *41*, 562–564. Bree, A.; Edelson, M. *Chem. Phys.* **1980**, *51*, 77–88.
(41) Dyck, R. H.; McClure, D. S. *J. Chem. Phys.* **1962**, *36*, 2326–2345.
(42) Warshel, A. *J. Chem. Phys.* **1975**, *62*, 214–221.
(43) Meič, Z.; Güsten, H. *Spectrochim. Acta Part A* **1978**, *34*, 101.
(44) Syage, J. A.; Felker, P. M.; Zewail, A. H. *J. Chem. Phys.* **1984**, *81*, 4685–4705.
(45) Suzuki, T.; Mikami, N.; Ito, M. *J. Phys. Chem.* **1986**, *90*, 6431–6440. Ito, M. *J. Phys. Chem.* **1987**, *91*, 517–526.
(46) Urano, T.; Maegawa, M.; Yamanouchi, K.; Tsuchiya, S. *J. Phys. Chem.* **1989**, *93*, 3459–3465.
(47) Kalinowski, H.-O.; Berger, S.; Braun, S. *Carbon-13 NMR Spectroscopy*; John Wiley and Sons: New York, 1988.
(48) Breitmaier, E.; Voelter, W. *^{13}C NMR Spectroscopy*, 2nd ed.; Verlag Chemie: Weinheim, Germany, 1978.
(49) Wehrli, F. W.; Marchand, A. P.; Wehrli, S. *Interpretation of Carbon-13 NMR Spectra*, 2nd ed.; John Wiley & Sons: New York, 1988.
(50) Krividin, L. B.; Kalabin, G. A. *Russ. Chem. Rev.* **1988**, *57*, 1–16.
(51) Marshall, J. L. *Carbon-Carbon and Carbon-Proton NMR Couplings*; Verlag Chemie International: Deerfield Beach, FL, 1983.
(52) Günther, H.; Herrig, W. *Chem. Ber.* **1973**, *106*, 3938–3950.
(53) Newton, D. M.; Schulman, J. M.; Manus, M. M. *J. Am. Chem. Soc.* **1974**, *96*, 17–23.

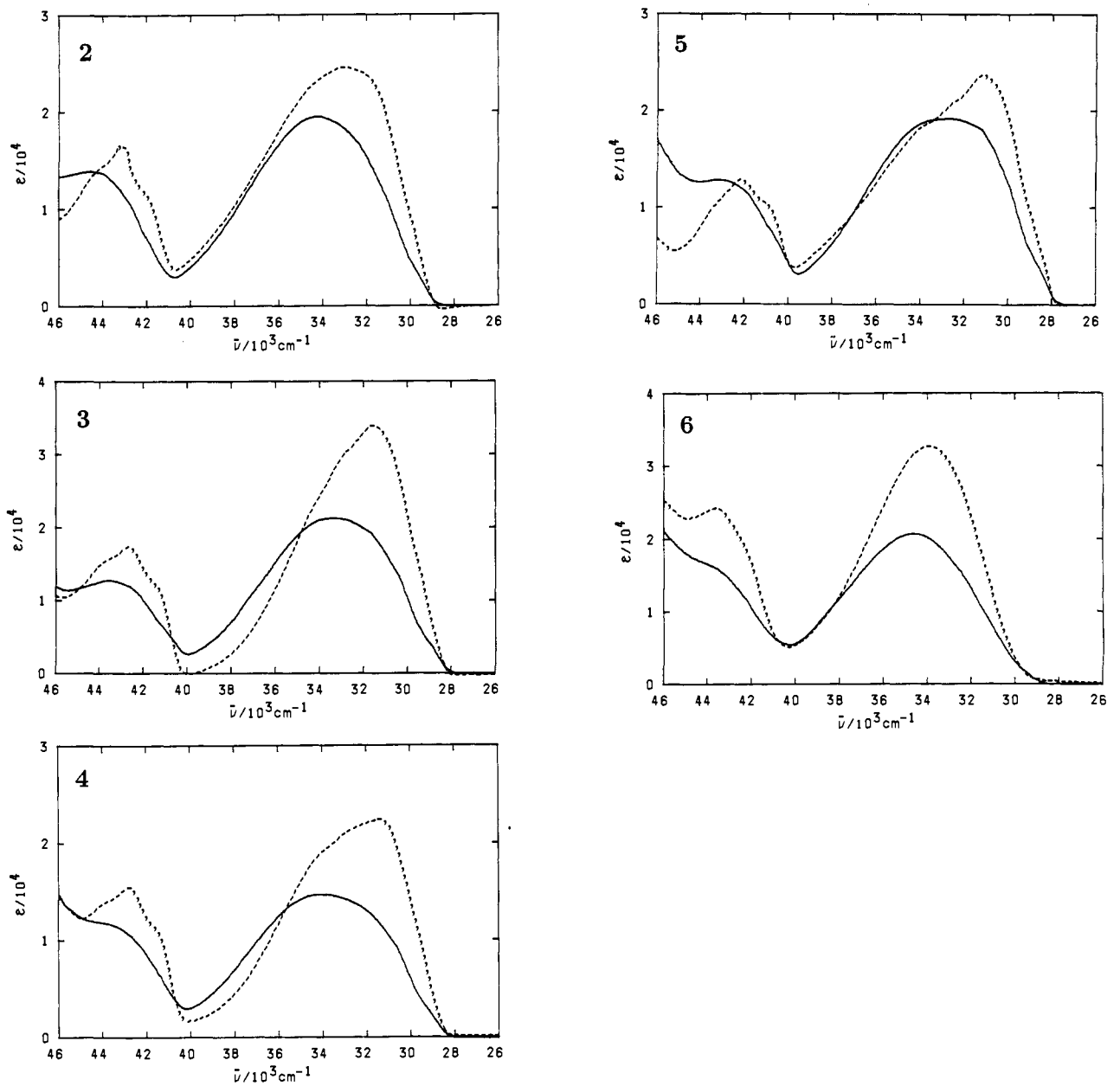

Figure 9. Electronic absorption spectra of **2–6** in 3-methylpentane solution. Solid and broken lines represent the spectra at 298 and at 77 K, respectively.

geometries of **2** and **4** at 298 K, the ^1J values were estimated by the use of eq 2 and 3, and the s character was calculated from the bond angles of Cα, as shown in Table IX.[54] Although the calculated ^1J values are only rough estimates, they show that the difference in ^1J(Cα,Cβ) between **2** and **4** at room temperature would amount to ca. 7 Hz and that of ^1J(Cα,Hα) ca. 13 Hz.

The proton nondecoupled ^{13}C NMR spectra of the ethylene carbons of (*E*)-2,2′-dimethyl[α,β-$^{13}C_2$]stilbene (^{13}C-**2**) and (*E*)-2,2′,5,5′-tetramethyl[α,β-$^{13}C_2$]stilbene (^{13}C-**4**) were measured[55] and successfully analyzed by assuming the AA′XX′YY′spin system, where Cα corresponds to A; Cβ, A′; Hα, X; Hβ, X′; H6, Y; H6′, Y′. The results are shown together with the literature data for (*E*)-[α,β-$^{13}C_2$]stilbene (^{13}C-**1**)[56-58] in Table X. The values of ^1J(Cα,Cβ) and ^1J(C,H) are in the range of the corresponding values reported for ethylenes.[47,52,59,60] Each *J* value of ^{13}C-**2** is nearly equal to the corresponding one of ^{13}C-**4** and ^{13}C-**1**. The NMR spectra did not show any significant change with lowering the temperature from 300 to 200 K. The results

Table XI. Data on Electronic Absorption Spectra of **2–6**

	obsd			calcd(MMP2-CNDO/S)		
compd	$\bar{\nu}_{max}$(10^3 cm^{-1})	ε(10^4)	*f*[a]	$\bar{\nu}_{max}$(10^3 cm^{-1})	*f*[a]	ω (deg)
2	34.2	1.94	0.600	34.1	1.05	25.6
3	33.3	2.13	0.653	33.3	1.12	25.8
4	34.0	1.47	0.478	33.7	0.85	26.0
5	32.6	1.92	0.617	33.0	0.96	25.6
6	34.6	2.07	0.616	34.3	1.02	30.8

[a] Oscillator strength.

(54) The bond angles of C1–Cα–Hα and Cβ–Cα–Hα of **2** were 114.5 ± 1.3 and 116.9 ± 1.3° in crystals at 298 K, respectively. Those of **4** were 114.6 ± 1.2 and 119.1 ± 1.2° in crystals at 298 K, respectively.

(55) Compounds ^{13}C-**2** and ^{13}C-**4** were prepared from the corresponding arylmagnesium bromide with *N*,*N*-dimethyl[^{13}C]formamide followed by coupling of the aldehyde (see the Experimental Section).

(56) Hansen, P. E.; Poulsen, O. K.; Berg, A. *Org. Magn. Reson.* **1976**, *8*, 632–637. Hansen, P. E.; Poulsen, O. K.; Berg, A. *Org. Magn. Reson.* **1979**, *12*, 43–49.

(57) Ernst, L. *Org. Magn. Reson.* **1984**, *22*, 789–791.

(58) Meić, Z.; Vikić-Topić, D.; Güsten, H. *Org. Magn. Reson.* **1984**, *4*, 237–244.

(59) Lynden-Bell, R. M.; Sheppard, N. *Proc. R. Soc. London, Ser. A* **1962**, *269*, 385–403.

(60) Graham, D. M.; Holloway, C. E. *Can. J. Chem.* **1963**, *41*, 2114–2118.

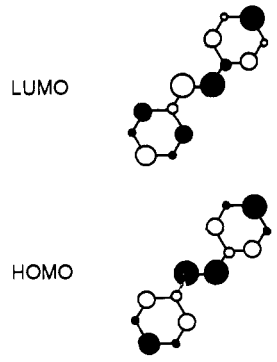

Figure 10. Relevant π molecular orbitals of (*E*)-stilbene in the planar form with C_{2h} symmetry.

suggest that there is no difference in d and θ between **2** and **4** in solution in the temperature range 200–300 K. It is, therefore, concluded that d and θ for **2–5** in solution hardly depend on the compound and the temperature in the range 200–300 K. It may also be concluded that d and θ for **1** in solution are nearly equal to the corresponding values for **2–5**.

UV Study. Electronic absorption spectra of **2–6** in solution are shown in Figure 9, and relevant data are listed in Table XI. The main absorption band of each compound at the lowest wavenumber is designated as band A, and only this band is discussed here.

As reported previously, band A can be ascribed mainly to a one-electron transition from the highest occupied π molecular orbital (HOMO) to the lowest unoccupied π molecular orbital (LUMO) (see Figure 10).[61,62] If bonds Cα–C1 and/or Cβ–C1′ are twisted, the HOMO is stabilized and the LUMO is destabilized. As a result, band A shifts to higher wavenumbers. When bond Cα–Cβ is twisted, band A, on the other hand, shifts to lower wavenumbers.

The magnitude of the electronic bathochromic effect of methyl substitution mainly depends on the absolute magnitude of the atomic orbital coefficient at the substitution position in the HOMO. The absolute magnitude of the atomic orbital coefficient increases in the order meta < ortho < para position, as shown in Figure 10. Hence, it is expected that $\bar{\nu}_{max}$ decreases in the order **2** > **4** ≈ **6** > **3** > **5**, if they have an identical geometry around the ethylene bond (d, θ, and $|\omega|$).

The results shown in Table XI agree with this prediction except for **6**, whose $\bar{\nu}_{max}$ value is the largest. The fact that the $\bar{\nu}_{max}$ value of **6** is larger than that of **2** is attributed to the buttressing effect of the methyl groups at the meta positions. It is therefore concluded that **2–5** have almost identical geometries around the ethylene bond and that $|\omega|$ of **6** is significantly larger than that of the other compounds in solution at room temperature. This is further supported quantitatively by the semiempirical SCF-MO-CI calculation using the program CNDO/S-CI,[63] as shown in Table XI. The MO calculations using the MMP2 structures as the input data reproduce $\bar{\nu}_{max}$ satisfactorily. The sequence of the calculated f's agrees with that of the observed ones, except for **2** and **5**, and with that of the molar absorption coefficient ϵ for all of the compounds.

As the temperature is lowered, band A shifts to significantly lower wavenumbers in all of the compounds. This is ascribed to the effect of an increase in the refractive index of the solvent[41] and to the change of the conformation. Since the red shift of band A for "stiff" stilbenes **11–13**, in which the (*E*)-stilbene skeleton is geometrically fixed by alkylene chains, is much smaller than that for **2–6**,[62] it is concluded that the $|\omega|$ values of **2–6** are appreciably decreased with lowering the temperature. However,

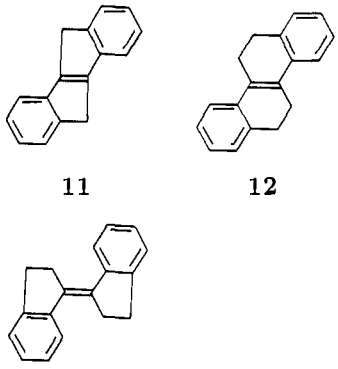

11 **12**

13

they still substantially deviate from 0° at 77 K, because band A of **2–6** ($\bar{\nu}_{max}$ (10^3 cm^{-1}) at 77 K: **2**, 33.03; **3**, 31.60; **4**, 31.51; **5**, 31.11; **6**, 33.97) is located at wavenumbers larger than those of stiff stilbenes (**11**, 29.85; **12**, 29.09; **13**, 29.14 10^3 cm^{-1} [62]) and does not show vibrational structure as observed for **1** and stiff stilbenes. In contrast to the geometry determined by X-ray diffraction, the geometry inferred from UV spectra is the equilibrium geometry. The observed change in the equilibrium geometry of **2–6** in solution should be ascribed to the increase in the viscosity of the solvent. Thus, the molecule is substantially flattened due to the rigid glass of the solution at 77 K.

Conclusion

This study has revealed that X-ray structures of the compounds having the (*E*)-stilbene skeleton commonly show an unusually short length for the central ethylene bond, while UV and NMR spectroscopic analyses in solution do not point to these anomalies. It is concluded that the short ethylene bond in the X-ray structures is an artifact caused by two kinds of disorders. One is the well-known static orientational disorder in the molecular plane, which was not detected in this study. The other is the dynamical disorder in a direction approximately perpendicular to the molecular plane which mainly originates from the torsional vibration of the C–Ph bonds, during which the movement of the benzene ring is restrained to a minimum. The characteristic temperature dependence of the ethylene bond length and angles and of the torsion angles of the C–Ph bonds is ascribed to the slight energy difference between the conformers, which interconvert due to the torsional vibration.

A similar dynamical disorder as well as an orientational disorder may be possible not only in (*E*)-stilbenes but also in various compounds such as diarylethylenes and diarylethanes. Shrinking of the bond which connects the two rigid groups and the temperature dependence of the geometry around the bond would commonly occur in the X-ray structures of these compounds.

Acknowledgment. We thank Professors Tosio Sakurai, Hiroshi Suzuki, and Shuji Tomoda for continuing encouragement, reading the manuscript, and valuable discussions and suggestions, and Professor Thomas Laube for suggesting the disorder model. K.O. is grateful to the Mitsubishi Oil Co. for financial support.

Registry No. (*E*)-**1**, 103-30-0; (*E*)-**2**, 36888-18-3; (*E*)-α,β-$^{13}C_2$-**2**, 138152-00-8; (*E*)-**3**, 51042-16-1; (*E*)-**4**, 82695-74-7; (*E*)-α,β-$^{13}C_2$-**4**, 138152-01-9; (*E*)-**5**, 138151-98-1; (*E*)-**6**, 15914-12-2; 2,4-$Me_2C_6H_4CHO$, 15764-16-6; 2,4,5-$Me_3C_6H_4CHO$, 5779-72-6; 2,3-$Me_2C_6H_4CHO$, 5779-93-1; 2-BrC_6H_4Me, 95-46-5; $H^{13}C(O)NMe_2$, 32488-43-0; 2-$MeC_6H_4{}^{13}CH(O)$, 138151-99-2; 2-bromo-*p*-xylene, 553-94-6.

Supplementary Material Available: Tables of crystal data, atomic coordinates, bond lengths and angles, anisotropic displacement parameters, molecular packing diagrams, and detailed data on the ^{13}C NMR spectra of ^{13}C-**2** and ^{13}C-**4** (62 pages); tables of observed and calculated structure factors (127 pages). Ordering information is given on any current masthead page.

(61) Suzuki, H. *Electronic Absorption Spectra and Geometry of Organic Molecules*; Academic Press: New York, 1967; Chapter 14.
(62) Ogawa, K.; Suzuki, H.; Futakami, M. *J. Chem. Soc., Perkin Trans. 2* **1988**, 39–43.
(63) Del Bene, J.; Jaffé, H. H.; Ellis, R. L.; Kuehnlenz, G. *QCPE174*.